www.rericjournal.ait.ac.th

# Comparison of the Spherical Optics and Fresnel Lens Performance in a Point-Focus CPV System

Carlo Renno*, [1], Alessandro Perone* and Valeria Pirone*

**ARTICLE INFO**

*Article history:*
Received 01 July 2021
Received in revised form
18 November 2021
Accepted 29 November 2021

*Keywords:*
Concentrating photovoltaic system
Energy and optical performance
Experimental point-focus system
Fresnel lens
Spherical optics

**ABSTRACT**

*The optical system is the component that more affects the performances of a Concentrating Photovoltaic (CPV) system. In this paper, a commonly used Fresnel lens and a less adopted spherical optics of the same diameter, are experimentally compared in a point-focus CPV system from an optical and an energy point of view. The spherical optics allows to reach the optical concentration factor and optical efficiency values equal respectively to 515 and 73%. These values are about three times higher with respect to the Fresnel lens, thus reducing the area of a CPV system with the same power output. Moreover, the spherical optics requires a lower accurate solar tracker with respect to the Fresnel lens, being the acceptance angle values equal respectively to 0.79° and 0.37°. The power and energy losses due to a solar tracking failure are also evaluated for both the optics. The concentration reached by the spherical optics allows also to increase the TJ cell temperature up to 65°C higher than the environmental temperature, and to obtain a cell electrical power equal about to 15 W. As for the Fresnel lens these values are much lower and equal respectively to about 40°C and 5 W. Moreover, the spherical mirror allows the electrical energy production for a longer time in case of a solar tracking failure.*

## 1. INTRODUCTION

The sun delivers to the Earth much more energy than humanity consumes [1]. However, an efficient and economic use of the solar energy is still a challenge [2]. The Concentrating Photovoltaic (CPV) systems allow to increase the solar energy use [3]. In a CPV system the solar radiation direct component [4] is concentrated by means of optical devices on highly efficient Multi-Junction (MJ) cells [5]. Hence, the use of expensive photovoltaic (PV) materials is proportionally reduced with the concentration factor and replaced with more convenient mirrors or lenses, thus reducing the overall cost of the system. Moreover, CPV systems are more environmentally friendly than traditional PV systems since they use less semiconductor components constituted by mined and rare metals [6]. However, CPV systems are still in a stage of development where new configurations, components and materials are tested to decrease the cost of energy obtainable [6]. More efficient optics and less expensive tracking and cooling systems need to be designed. In particular, the optical system has the greatest impact on the CPV system energy and economic performances [7]. In fact, a well-designed optical system can significatively improve the achievable concentration factor, thus reducing the necessary semiconductor components and then the costs with the same power output. Moreover, the secondary optics can improve the acceptance angle and optical tolerance of a CPV system, thus allowing the use of cheaper solar trackers. Several types of optical systems have been developed and differ according to geometry, levels of concentration, *etc.*; each optics presents advantages and disadvantages. According to their principle of operation, the optical systems can be refractive and reflective [8]. Another classification is related to the achievable level of concentration: low (<10 suns), medium (10–100 suns), high (100–2000 suns) and ultrahigh (2000-42000 suns) [9]. Depending on the sunlight is conveyed on a small or larger area or along a line, the optical systems can be classified in point-focus, dense array and line-focus [10]. As for the point-focus optical systems, most applications use refractive optics and above all the Fresnel lens [3]. An interesting analysis of the experimental methods used to evaluate the optical performances of a Fresnel lens, is reported in [11]. In [12] a Fresnel lens focuses the sunlight on a plano-concave lens that works as secondary optics to uniform the concentrated solar radiation on the surface of a Multi-Junction (MJ) solar cell. Electrical and thermal parameters are analyzed in [13] to evaluate the potential energy production of a CPV system which uses a Fresnel lens as primary optics. On the contrary, point-focus reflective optics are not much diffused. An interesting configuration, made up of a double reflection Cassegrain CPV system [14] with parabolic dish and hyperbolic mirror, is studied in [15].

* Department of Industrial Engineering, University of Salerno, Via Giovanni Paolo II, 132, 84084 Fisciano (Salerno), Italy.

[1]Corresponding author;
Tel: + 39 089964327, Fax: + 39 089964037.
E-mail: crenno@unisa.it

A point-focus CPV system that adopts a parabolic mirror as primary optics, has been analyzed in [16]. However, reflective optics are above all used in dense-array [17]-[18] or line-focus [19]-[20] configurations. Although the reflective point-focus optics are not very diffused [21], they present a good potentiality to increase the performances of a CPV system [22]. Hence, the novelty of this paper is to compare two different typologies of point-focus optics [23] with the same diameter: a less used spherical mirror and a commonly adopted Fresnel lens. From a study commissioned by the authors it has been evidenced that, considering the small size of TJ solar cell, a spherical mirror is to be preferred to a parabolic one from a technical-economic point of view. In fact, even if it requires a secondary optics to overcome the spherical aberration, the total cost of such optical system is about 60% lower with respect to a parabolic mirror of the same dimensions because it is easier to produce. After the analysis of the optical performances of Fresnel lens and mirror, the energy performances that these systems would guarantee in a point-focus CPV system [24], are investigated and compared in this paper.

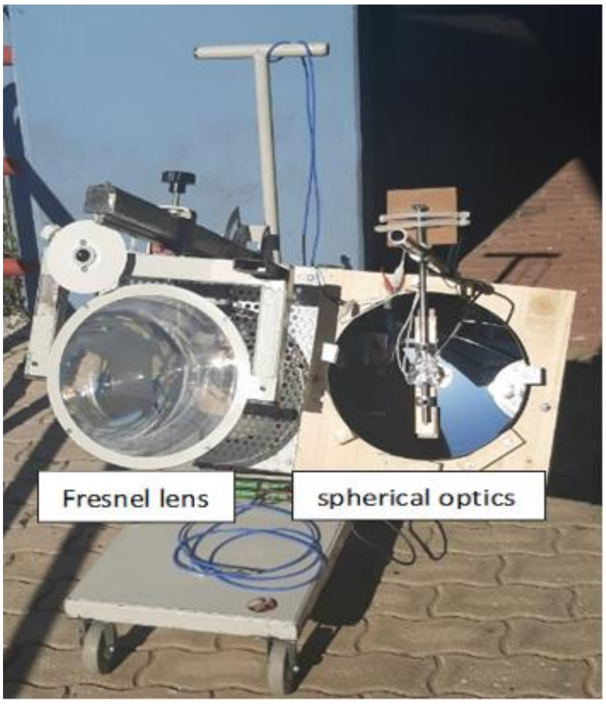


**Fig. 1. Photo of the experimental CPV system.**

**Table 1. Parameters of the Triple-Junction cell.**

| *parameter* | *value* |
|---|---|
| material | InGaP/InGaAs/Ge |
| dimensions | 10.0 mm x 10.0 mm |
| $\eta_r$ (at 25°C, 50 W/cm$^2$ – 1000 suns) | 39.0% |
| Temperature coefficient ($\sigma_t$) | -0.04%/K |
| $V_{oc}$ (at 25°C, 50 W/cm$^2$ – 1000 suns) | 2.94 V |
| $I_{sc}$ (at 25°C, 50 W/cm$^2$ – 1000 suns) | 4.49 A |

## 2. EXPERIMENTAL POINT-FOCUS CPV SYSTEM

The experimental CPV plant (Figure 1) has been realized at the Applied Thermodynamics Laboratory of University of Salerno (Italy). It is a point-focus CPV system that presents primary optics both reflective and refractive. The refractive optics is a Fresnel lens in PMMA, with thickness and diameter equal respectively to 0.4 cm and 30 cm. The reflective optics consists of a spherical mirror of diameter 30 cm. It has been subjected to a protected aluminizing treatment to reflect the solar radiation within the Triple-Junction (TJ) cell operating wavelength range. Both the primary optics convey the solar radiation on a receiver consisting of a TJ solar cell and a passive cooling system. The TJ cell, constituted by InGaP/GaAs/Ge, is the same for each receiver and presents an area equal to 10.0×10.0 mm$^2$ (Table 1). A pyramid-shaped light-guide, with areas respectively equal to 16.0×16.0 mm$^2$ and 10.0×10.0 mm$^2$ and height of 75 mm, is adopted as secondary optics for each TJ cell. It allows to uniform the concentrated solar radiation coming from spherical mirror and Fresnel lens to avoid problems respectively of spherical aberration and chromatic aberration, and to improve the optical efficiency. A tracking system is used in the experimental CPV system to converge the maximum Direct Normal Irradiance (DNI) on the receiver.

The experimental plant presents three freedom degrees allowing both the solar tracking and the concentration factor variation. The first two allow the solar tracking in the horizontal plane to follow the sun in the azimuth direction and in the vertical plane to follow the sun in the zenithal direction. Moreover, it is possible to vary the distance between primary optics, placed perpendicularly to the sunrays, and receiver; so, the focal length is considered as further freedom degree in the experimental tests. The experimental plant allows to move on a vertical axis the receiver in the case of reflective optics and the Fresnel lens in the refractive case. Hence, the solar radiation incident on the TJ cell can be varied modifying the optical concentration factor. The experimental plant presents PT100 thermo-resistances (accuracy of ±0.2°C) used to measure the TJ cells and outdoor temperatures and a pyrheliometer (accuracy of 2%) to measure the DNI (Figure 2).

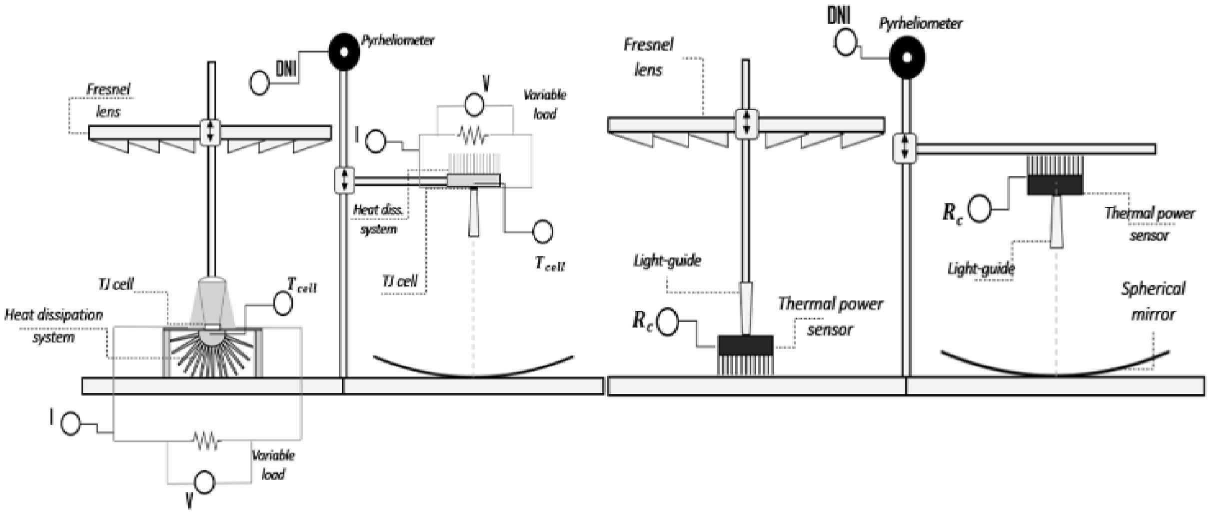


**Fig. 2. Plant scheme with the measurement instruments of the energy performances (a) and of the optical performances (b).**

A variable electrical load is linked to each TJ cell and an acquisition data system is used for the experimental measurements of voltage, current, DNI and temperatures. The optical concentration factor has been experimentally calculated as ratio between solar radiation concentrated on the TJ cell and DNI that represents the incident power flow on the optical system. So, the optical concentration factor depends only on the system optical performances and is independent from the TJ cell electrical performance. The solar radiation concentrated has been measured by means of a thermal power sensor (accuracy of ±3%) that presents a series of bimetallic junctions (thermopile), and the thermal flow through the sensor determines a voltage proportional to the power absorbed when it flows into the thermopile. A calibration of the thermal power sensor has been realized to compare the measurements coming from the two sensors. It is necessary that the solar radiation concentrated on TJ cell and power sensor, are the same (Figure 2) during the measurement of the optical concentration factor.

## 3. OPTICAL AND ENERGY PERFORMANCES

The main aim of this paper is to compare two different typologies of primary optics with the same diameter, spherical mirror and Fresnel lens, adopting the experimental point-focus CPV system above presented. The energy producibility of a CPV system depends on the amount of solar radiation concentrated on the TJ cells; so, the optical performances have a direct impact on the energy ones [25]. Hence, first an accurate analysis of the optical performances of each system is performed and, successively, the energy performances, that both optical systems have to guarantee in a point-focus CPV system, are experimentally compared.

First, the maximum optical performances obtained by two optical systems have been measured and compared. Successively, the precision required to the solar tracking system in terms of acceptance angle and losses due to a solar tracking failure, has been experimentally evaluated for both the optical systems also considering the influence of a secondary optics. Finally, the electrical and thermal performances that each optical system allows to obtain in a point-focus

CPV system, have been evaluated. The experimental measurements have been carried out in January and February 2020 at Fisciano (Italy) considering a sampling interval of 15 s during the data acquisition.

### 3.1 Optical Performances Comparison

The main parameter that characterizes an optical system is its optical concentration factor ($C_{opt}$), defined as ratio between the solar radiation concentrated on the TJ cell ($R_c$) and the DNI that represents the power flow incident on the optical system. The upper limit of $C_{opt}$ is the geometrical concentration ratio ($C_{geo}$), defined as ratio between the solar concentrator area ($A_{conc}$) perpendicular to the sunrays and the TJ cell area ($A_c$). Because the two optical systems considered present the same dimensions, $C_{geo}$ is the same for both. The optical efficiency ($\eta_{opt}$), that considers the actual power incident on the concentrator that reaches the receiver, is equal to:

$$\eta_{opt} = \frac{C_{opt}}{C_{geo}} \quad (1)$$

In order to obtain the maximum value of $C_{opt}$ and $\eta_{opt}$, the distance between each optics and the receiver, and then the focal length, has been opportunely set during the experimental analysis. Hence, the trend of $C_{opt}$ as function of $h_{M-C}$ (distance between spherical mirror and TJ cell) and $h_{L-C}$ (distance between Fresnel lens and TJ cell) has been analyzed for both optics with light-guide.

In presence of the light-guide, it has been noted that for both optics $C_{opt}$ increases respectively with $h_{L-C}$ and $h_{M-C}$ until it reaches its maximum value corresponding to the proper focal length of each optics ($h_{L-C,max}$ and $h_{M-C,max}$). This increase can be described for the Fresnel lens by an exponential trend and for the spherical mirror by a parabolic trend, respectively given by the Equations 2 and 3:

$$C_{opt} = Ae^{Bh_{L-C}} \quad (2)$$

$$C_{opt} = C{h_{M-C}}^2 + Dh_{M-C} + E \quad (3)$$

On the contrary, for values of $h_{L-C}$ and $h_{M-C}$ higher than their respective optimal values, $C_{opt}$ decreases in a parabolic way that can be described by the Equation 3 for the spherical mirror and by the following equation for the Fresnel lens:

$$C_{opt} = C{h_{L-C}}^2 + Dh_{L-C} + E \quad (4)$$

The coefficients of the Equations 2, 3 and 4 have been experimentally determined. Without light-guide, the growing trends would be similar to the previous case (Equations 2 and 3) but with different coefficients values. On the contrary, in the range of $h_{L-C}$ and $h_{M-C}$ higher than their respective optimal values, the secondary optics absence leads to a faster decay of $C_{opt}$that results exponential for both optics. The trends of $\eta_{opt}$ and $C_{opt}$ are the same because differ only by a multiplicative factor.

An accurate comparison between different optical systems cannot be based only on the $C_{opt}$ value, but a more detailed analysis is necessary. An important parameter is the accuracy that each optics requires to the solar tracker to avoid high power losses. For this purpose, an important parameter is the acceptance angle ($\theta$) that represents the angle between sun direction and normal to the optical system, for which the incident radiation is reduced to 90% in comparison with its maximum value. In fact, the optical systems with low values of $\theta$ require very accurate tracking systems to avoid a fast reduction of the optical performances. Hence, the concentrated power reduction in terms of the misalignment angle ($\theta_{mis}$) between sun direction and normal to each concentrator, has been experimentally analyzed. Moreover, the concentrated power decrease due to a solar tracking failure has been evaluated for both optics.

### 3.2 Energy Performances Comparison

The optical characteristics, and above all $C_{opt}$, affect directly the CPV system energy performances. In particular, the TJ cell temperature ($T_c$) increase when it is submitted to solar concentration, has been evaluated. The $T_c$ evaluation is fundamental because it affects the TJ cell electrical efficiency and then the CPV system electrical producibility. Moreover, it affects the quality of the recovered thermal energy when an active cooling system is used in the CPV/T systems.

Once fixed the maximum value of $C_{opt}$ for each optics, the $T_c$ increase compared to the environmental temperature ($T_{env}$) when the DNI varies, has been evaluated; hence, the $T_c$ increase has been determined when the TJ cell is submitted to solar concentration and $T_{env}$ varies. The experimental results have shown that the $T_c$ increase with respect to $T_{env}$ raises logarithmically with DNI:

$$T_c - T_{env} = F \cdot \log(Rc) + G \quad (5)$$

where the parameters F and G have been experimentally determined for each optics.

A similar analysis has been realized for the TJ cell electrical power ($P_{el,c}$). It has been experimentally evidenced that $P_{el,c}$ increases linearly with DNI according to the following equation:

$$P_{el,c} = \alpha \cdot R_c + \beta \quad (6)$$

where $\alpha$ and $\beta$ have been experimentally determined for each optics.

Finally, the total electric energy produced by the TJ cell has been also evaluated for each optical system in cases of correct and incorrect solar tracking.

## 4. RESULTS AND DISCUSSION

The energy and optical performances of a CPV system are strictly connected to each other and depend on the optical system chosen. Hence, the experimental results obtained for the two different optics analyzed in this paper, are compared and discussed in the following sections.

### 4.1 Results of the Optical Comparison

The main parameter that characterizes an optical system is $C_{opt}$. The trends of $C_{opt}$ experimentally measured for Fresnel lens and spherical optics are reported in Figure 3 in terms of the distance between receiver and concentrator. It can be observed that the maximum values of $C_{opt}$ are respectively equal to 171 and 515 for Fresnel lens and spherical mirror. So, corresponding to the same size, the Fresnel lens is characterized by greater power losses resulting in a $C_{opt}$ which is about 67% lower than the spherical optics.

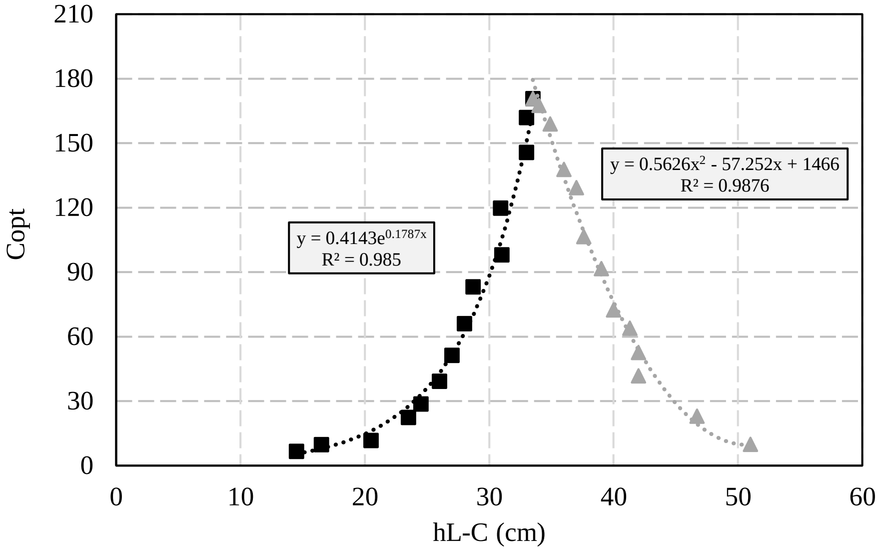


(a)

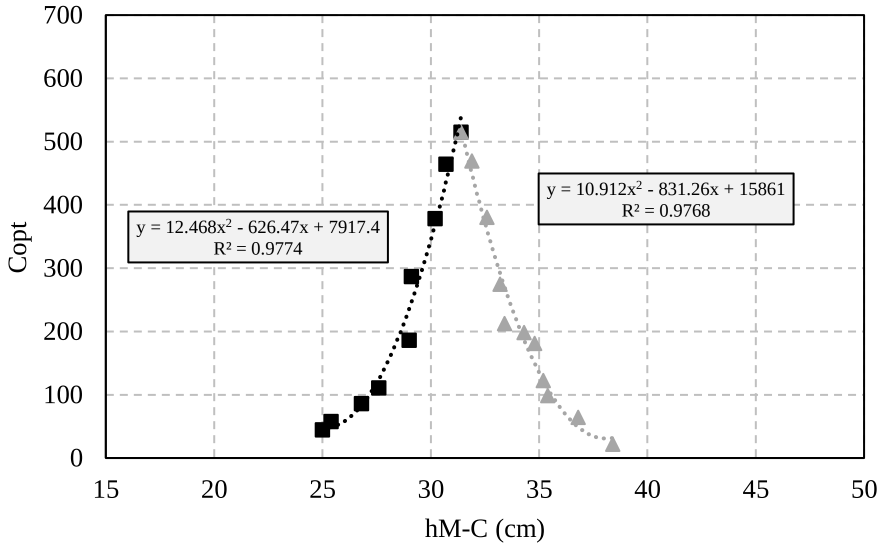


(b)

**Fig. 3. Trends of $C_{opt}$ as function of the distance between optics and receiver in the case of Fresnel lens (a) and spherical mirror (b) in presence of secondary optics.**

**Table 2. Coefficients values of the experimental equations describing the trends of $C_{opt}$.**

| *Case* | A | B | C | D | E | *R²* |
|---|---|---|---|---|---|---|
| (a): $h_{L-C} < h_{L-C,max}$ | 0.41 | 0.18 | - | - | - | 0.9794 |
| (a): $h_{L-C} > h_{L-C,max}$ | - | - | 0.562 | -57.3 | 1466 | 0.988 |
| (b): $h_{M-C} < h_{M-C,max}$ | - | - | 12.5 | -627 | 7917 | 0.977 |
| (b): $h_{M-C} > h_{M-C,max}$ | - | - | 12.2 | -921 | $1.738 \cdot 10^4$ | 0.970 |

The coefficients values of the experimental equations describing the trend of $C_{opt}$ are reported in Table 2 for the Fresnel lens (a) and the spherical mirror (b). In particular, $h_{L-C,max}$ is equal to 33.5 cm in the case (a) and to 25.5 cm in the case (b) for the Fresnel lens; referring to the spherical mirror, $h_{M-C,max}$ is equal to 31.4 cm in the case (a) and to 23.9 cm in the case (b).

Considering that both optics have the same diameter equal to 30 cm and convey the solar radiation on a TJ cell of 10x10 mm$^2$, they present the same $C_{geo}$ equal to 707. Hence, the comparison between the $C_{geo}$ and $C_{opt}$ values of each optical system is reported in Figure 4. Moreover, in Figure 5 it can be noted that the optical efficiency of the spherical mirror, equal to 73%, is significantly higher than $\eta_{opt}$ of the Fresnel lens equal to 24%. This is due to the high difference between the values of the optical concentration factors.

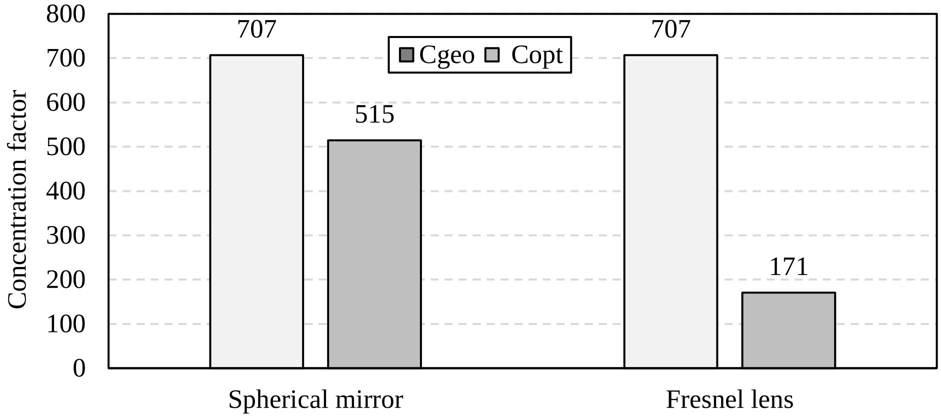


**Fig. 4. Comparison between the optical and geometrical concentration factor for the two optics.**

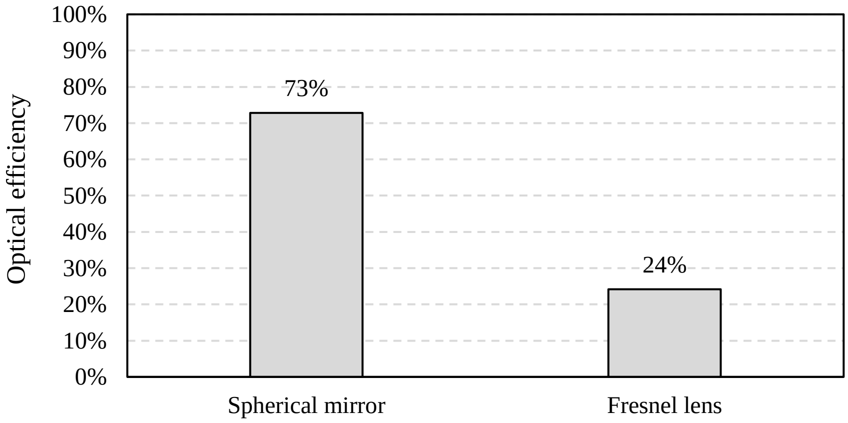


**Fig. 5. Comparison between the optical efficiencies of the two optics.**

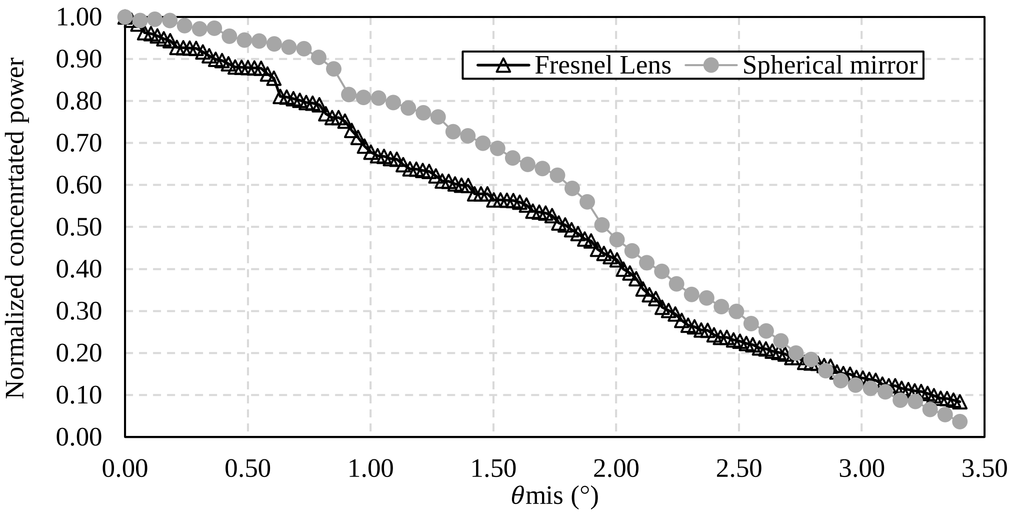


**Fig. 6. Reduction of the normalized concentrated power as function of the misalignment angle for both the optics.**

In order to evaluate the accuracy that each optical system requires to the solar tracker, the acceptance angle (θ) has been determined. For this purpose, the measured values of concentrated power normalized with respect to the maximum value, are reported for both optics in

Figure 6 in terms of the misalignment angle ($\theta_{mis}$). In Figure 6, the acceptance angle can be determined as the value of the misalignment angle ($\theta_{mis}$) for which the concentrated power reaches the 90% of its initial value. Hence, as shown in Figure 6, the spherical optics is characterized by a higher value of the acceptance angle, equal to 0.79°, while for the Fresnel lens it is equal to only 0.37°. This means that a spherical optics requires a lower accurate solar tracker with respect to the Fresnel lens. Moreover, in Figure 6 it can be also noted for both optics that, for a misalignment angle of about 3.40°, the solar radiation concentrated on the receiver is near to zero.

It is also interesting to evaluate the reduction over time of $C_{opt}$ when there is a solar tracking failure; the results of this analysis are shown in Figure 7 for both optics. The concentration level decrease is almost linear for both the optics. It can be noted that the optical concentration factor is halved after about 435 s and 510 s, and it is near to zero after about 885 s and 1040 s for the Fresnel lens and the spherical optics respectively.

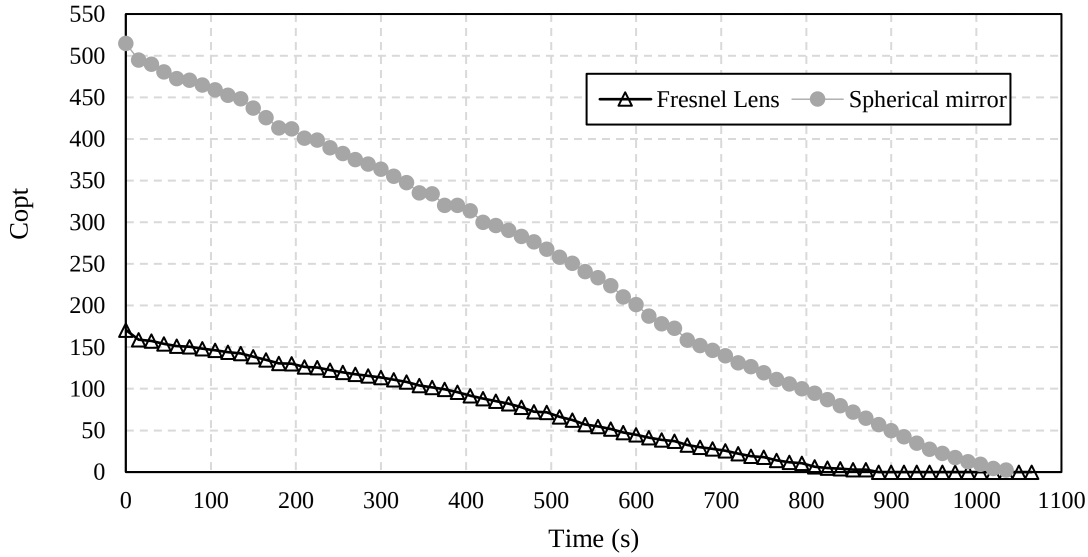


**Fig. 7. Reduction over time of the optical concentration factor due to a solar tracking failure for both the optics.**

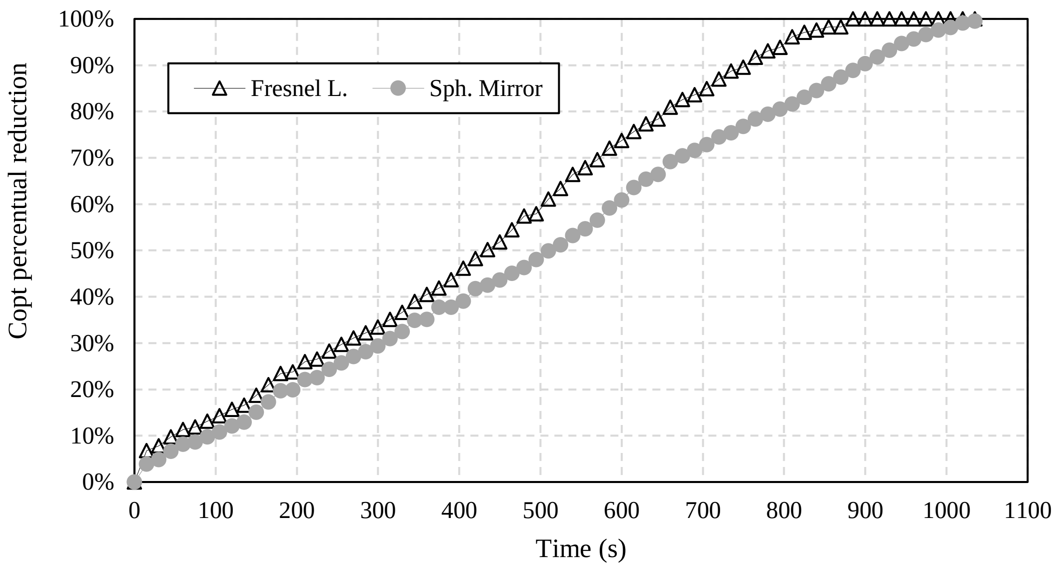


**Fig. 8. Percentual reduction over time of the optical concentration factor for the two optics**

The two trends reported refer to different initial values of $C_{opt}$ . Hence, in order to make them comparable, it would be more interesting to analyze the percentual reduction over time of the optical concentration factor. As shown in Figure 8, the two trends are similar but the percentual reduction of $C_{opt}$ is more marked in the case of the Fresnel lens. In fact, as seen also in Figure 6, a misalignment between sun direction and normal to the optical system determines greater power losses in the case of the Fresnel lens.

### *4.2 Results of the Energy Comparison*

First, from the thermal energy point of view, the TJ cell temperature increase under concentration has been evaluated for two optical systems. In Figure 9 the increase of $T_c$ compared to $T_{env}$ when DNI varies, and in correspondence of the maximum value of $C_{opt}$ of each optics, is shown. It can be noted that the increase of $T_c$ with respect to $T_{env}$ increases logarithmically with DNI for both cases. The higher level of concentration obtained by the spherical optics allows to reach higher values of $T_c$, up to about 65°C higher than $T_{env}$ for a DNI equal to about 900 W/m$^2$. As for the Fresnel lens the maximum increase of $T_c$ is about 40°C higher than $T_{env}$. The equations experimentally determined allow to evaluate the temperatures that can be reached by the TJ cell in correspondence of the two optical systems analyzed in each locality, once known the values of DNI and $T_{env}$. Hence, if an active cooling system [26] is used it is possible to recover thermal energy whose quality is strictly dependent on the TJ cells temperature. Moreover, $T_c$ highly affects the TJ cell electrical efficiency, and then its evaluation is necessary to evaluate the CPV system electrical producibility.

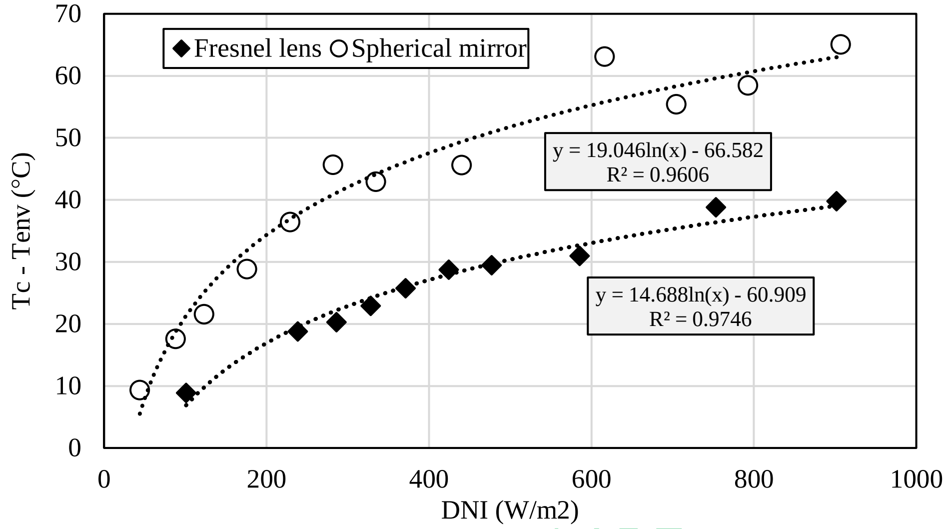


**Fig. 9. Increase of the TJ cell temperature as function of DNI for the two optics.**

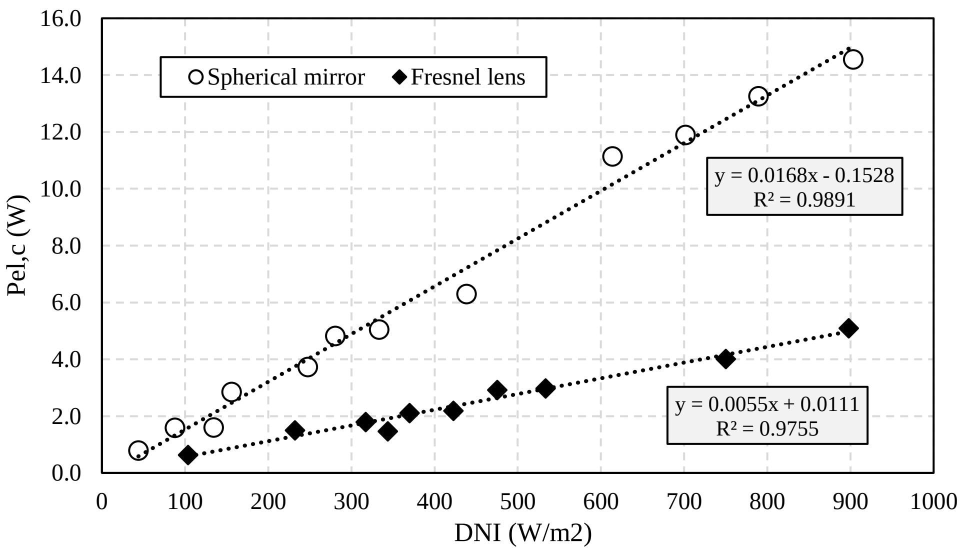


**Fig. 10. Increase of the TJ cell electrical power as function of DNI for the two optics**

**Table 3. Coefficients values of the experimental equations describing the trends of $T_c$ and $P_{el,c}$.**

| Equation | *F* | *G* | *α* | *β* | $R^2$ |
|---|---|---|---|---|---|
| (5) Fresnel Lens | 14.69 | -60.91 | - | - | 0.975 |
| (5) Spherical Mirror | 19.03 | -66.52 | - | - | 0.961 |
| (6) Fresnel Lens | - | - | 0.0055 | 0.0111 | 0.976 |
| (6) Spherical Mirror | - | - | 0.0168 | -0.1528 | 0.989 |

From the electrical energy point of view, the increase of the TJ cell electrical power $P_{el,c}$ with DNI has been evaluated for both optics. As shown in Figure 10, $P_{el,c}$ increases approximately linearly with DNI , reaching a maximum value of about 15 W and 5 W for the spherical mirror and the Fresnel lens respectively in correspondence of DNI equal to 900 W/m$^2$.

It can be noted that these data refer to thermal regime conditions, so the registered value of $P_{el,c}$ takes into account the electrical efficiency reduction due to the cell temperature. The coefficients values of the experimental equations related to the trends of $T_c$ and $P_{el,c}$, are reported in Table 3 for the Fresnel lens and the spherical mirror.

Moreover, in order to underline the influence that the optical performances have on the electrical producibility, it should be useful to analyze the trend of the cumulative electric energy produced by the TJ cell in a time interval of 1200 s in correspondence of correct and incorrect solar tracking for both optics (Figure 11). These trends refer to a DNI of about 900 W/m$^2$ and $C_{opt}$ equal to its maximum value for each optics. It can be noted that the decay of $C_{opt}$ (Figure 7) due to a solar tracking failure, leads to a high decrease of the TJ cell electrical producibility. After about 990 s in the case of the spherical optics and 780 s in the case of the Fresnel lens, the TJ cell does not produce more electrical energy. After the interval time of 1200 s, there is a decrease of the cumulative electrical energy equal to about 59% and 65% respectively for mirror and lens.

Finally, considering the maximum values of the TJ cell electrical power shown in Figure 10, it is possible to calculate, as first approximation, the number of optics ($N_{opt}$) and the relative necessary area ($A_{opt}$) for a CPV plant with a peak electrical power of 3.5 kW that could match the electrical requirements of a residential user (Figure 12). It can be noted that, despite the optics have the same dimensions, a higher optical efficiency allows to reduce the number of optical systems necessary and then their area at the same electrical output.

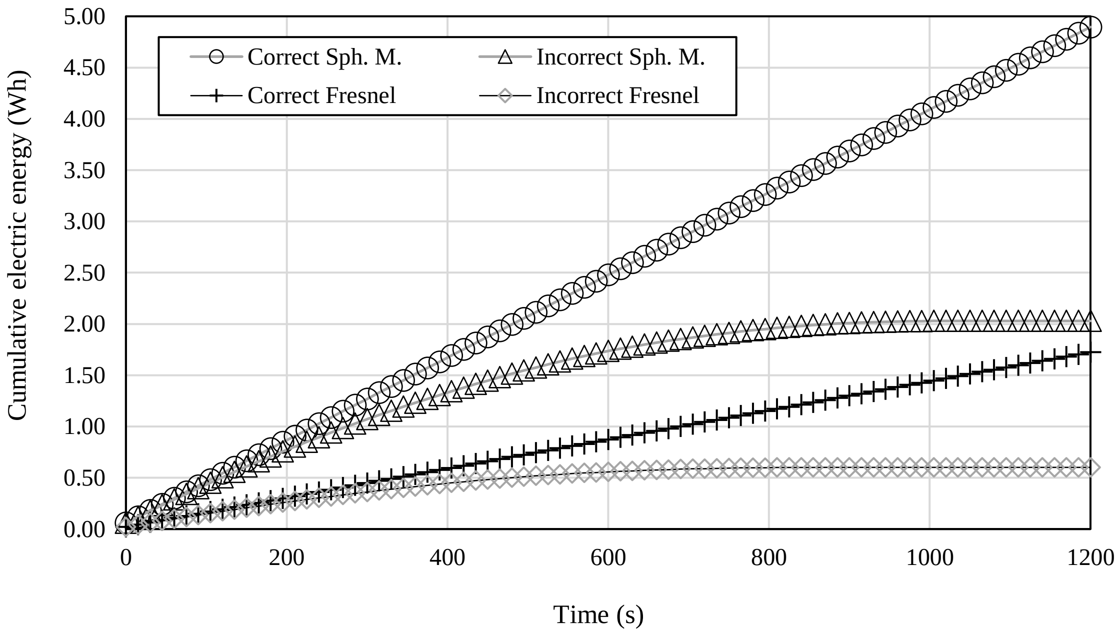


**Fig. 11. Cumulative electrical energy produced in the cases of a correct solar tracking and of a failed solar tracking for the two optics.**

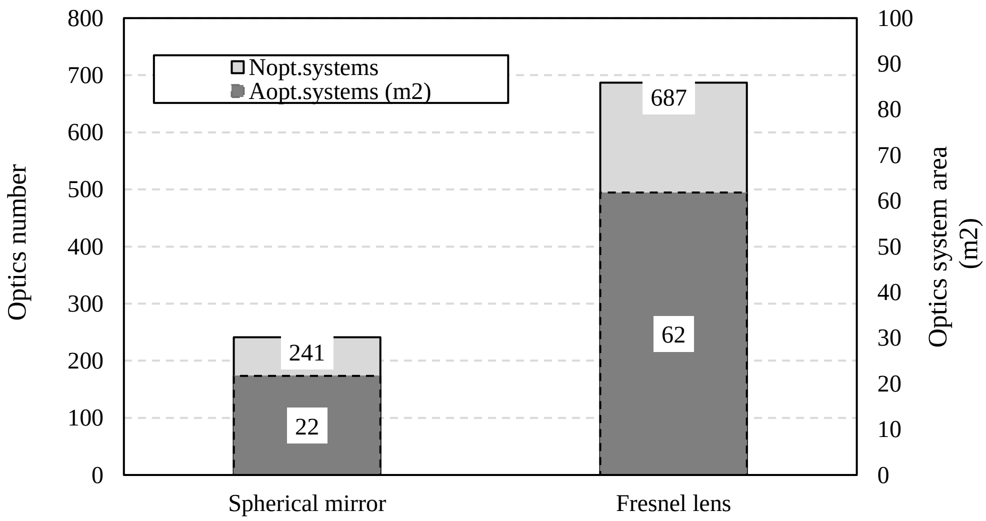


**Fig. 12. Number of optics and the relative necessary area of a CPV system adopted for a residential user.**

## 5. CONCLUSION

The main novelty of this paper has been to compare, from an optical and an energy point of view, two different types of primary optics with the same diameter, adopted in a point-focus CPV system: the less used spherical optics and the more used Fresnel lens.

As for the optical comparison, the results have shown that the spherical mirror allows to obtain values of $C_{opt}$ and $\eta_{opt}$ equal respectively to 515 and 73%. These values are about three times higher with respect to the Fresnel lens. Moreover, a spherical mirror requires a less accurate solar tracker with respect to the Fresnel lens, with values of the acceptance angle equal respectively to 0.79° and 0.37°. The absolute and percentual reduction over time of $C_{opt}$ in case of a solar tracking failure, has been also investigated for both optics. Despite similar trends, in the case of the Fresnel lens $C_{opt}$ is near to zero about 155 s before than the spherical mirror.

As for the energy comparison, the higher levels of concentration achievable by the spherical mirror allow to increase $T_c$ up to about 65°C higher than $T_{env}$ for a DNI equal to about 900 W/m$^2$. This increase is lower for the Fresnel lens and equal to about 40°C. In both cases the increase of $T_c$ with DNI follows a parabolic trend. Referring to the electrical aspects, the increase of $P_{el,c}$ with DNI is approximately linear, with a maximum value of about 15 W and 5 W for spherical mirror and Fresnel lens respectively. The trends of the cumulative electric energy produced by the TJ cell with both the optical systems, have been evaluated also in case of a solar tracking failure, with a production decrease of 58.9% and 65.1%, respectively for the spherical mirror and the Fresnel lens. Finally, because of its higher optical efficiency, the use of spherical optics allows to reduce the number of optical systems and the relative necessary area with respect to the Fresnel lens in correspondence with the same electrical output.

## NOMENCLATURE

| | |
|---|---|
| A | area (m$^2$) |
| $C_{geo}$ | geometrical concentration factor |
| $C_{opt}$ | optical concentration factor |
| CPV | Concentrating Photovoltaic system |
| CPV/T | Concentrating Photovoltaic and Thermal system |
| DNI | Direct Normal Irradiance (W/m$^2$) |
| $h_{M-C}$ | spherical mirror-TJ cell distance (m) |
| $h_{L-C}$ | Fresnel lens-TJ cell distance (m) |
| $I_{sc}$ | short circuit current (A) |
| N | number |
| P | electric power (W) |
| $R_c$ | concentrated solar radiation (kW/m$^2$) |
| T | temperature (°C) |
| TJ | Triple-Junction |
| $V_{oc}$ | open circuit voltage (V) |
| $\eta$ | efficiency |
| $\Theta$ | angle (°) |
| *Subscripts* | |
| c | cell |
| conc | concentrator |
| el | electrical |
| env | environmental |
| opt | optical, optics |
| mis | misalignment |

## REFERENCES


[1] Soni M.S. and N. Gakkhar. 2014. Techno-economic parametric assessment of solar power in India: A survey. *Renew Sustain Energy Rev* 40: 326-34.

[2] Rejeb O., Shittu S., Ghenai C., Li G., Zhao X., and Bettayeb M., 2020. Optimization and performance analysis of a solar concentrated photovoltaic-thermoelectric (CPV-TE) hybrid system. *Renewable Energy* 152: 1342-1353.

[3] Bellos E., Tzivanidis C., Antonopoulos K.A., and Gkinis G., 2016. Thermal enhancement of solar parabolic trough collectors by using nanofluids and converging-diverging absorber tube. *Renewable Energy* 94: 213-222.

[4] Amrouche B. and X. Le Pivert. 2014. Artificial neural network based daily local forecasting for global solar radiation. *Applied Energy* 130: 333–41

[5] Renno C., Petito F., Landi G., and Neitzert H.C., 2017. Experimental characterization of a concentrating photovoltaic system varying the light concentration. *Energy Conversion and Management* 138:119-130.

[6] Shanks K., Senthilarasu S., and Mallick T.K., 2016. Optics for concentrating photovoltaics: Trends, limits and opportunities for materials and design. *Renewable and Sustainable Energy Reviews* 60: 394–407.

[7] Renno C., 2018. Experimental and theoretical analysis of a linear focus CPV/T system for cogeneration purposes. *Energies* 11: article number 2960.

[8] Han X., Zhao G., Xu C., Ju X., Du X., and Yang Y., 2017. Parametric analysis of a hybrid solar concentrating photovoltaic/concentrating solar power (CPV/CSP) system. *Applied Energy* 189: 520-533.

[9] Chemisana D. and T. Mallick. 2014. Building integrated concentrated solar systems. Solar energy sciences and engineering applications. N. Enteria, A. Akbarzadeh, Eds. CRC Press: 545-788.

[10] Serrano-Aguilera J.J., Valenzuela L., and Fernandez-Reche J., 2016. Inverse Monte Carlo Ray-Tracing method (IMCRT) applied to line-focus reflectors. *Solar Energy* 124: 84-197.

[11] Victoria M., Askins S., Herrero R., Antón I., and Sala G., 2016. Assessment of the optical efficiency

of a primary lens to be used in a CPV system. *Solar Energy* 134: 406-415.

[12] Tien N.X. and S. Shin. 2016. A novel concentrator photovoltaic (CPV) system with the improvement of irradiance uniformity and the capturing of diffuse solar radiation. *Applied Sciences* 6(9): 251.

[13] Renno C. and F. Petito. 2018. Triple-junction cell temperature evaluation in a CPV system by means of a Random-Forest model. *Energy Conversion and Management* 169: 124-136.

[14] Burhan M., Shahzad M.W., and Ng K.C., 2017. Long-term performance potential of concentrated photovoltaic (CPV) systems. *Energy Conversion and Management* 148:90-99.

[15] Kim Y., Jeong H.J., Kim W., Chun W., Han H.J., and Lim S.H., 2017. A comparative performance analysis on daylighting for two different types of solar concentrators: Dish vs. Fresnel lens. *Energy* 137: 449-456.

[16] Bonsignore G., Gallitto A.A., Agnello S., Gelardi F.M., Sciortino L., Collura A., Lo U., Milone S., Montagnino F.M., Paredes F., and Cannas M. CHP efficiency of a 2000 CPV system with reflective optics. *AIP Conference Proceedings*, 1–5.

[17] Flitsanov Y. and A. Kribus. 2018. A cooler for dense-array CPV receivers based on metal foam. *Solar Energy* 160: 25-31.

[18] Fernández Á., Laguna G., Rosell J., Vilarrubí M., Ibañez M., Sisó G., and Barrau J., 2018. Assessment of the impact of non-uniform illumination and temperature profiles on a dense array CPV receiver performance. *Solar Energy* 171: 863-870.

[19] Yazdanifard F., Ebrahimnia-Bajestan E., and Ameri M., 2017. Performance of a parabolic trough concentrating photovoltaic/thermal system: effects of flow regime, design parameters, and using nanofluids. *Energy Conversion and Management* 148:1265-1277.

[20] Widyolar B., Jiang L., Abdelhamid M., and Winston R., 2018. Design and modeling of a spectrum-splitting hybrid CSP-CPV parabolic trough using two-stage high concentration optics and dual junction InGaP/GaAs solar cells. *Solar Energy* 165: 75-84.

[21] Wang G., Chen Z., Hu P., and Cheng X., 2016. Design and optical analysis of the band-focus Fresnel lens solar concentrator. *Applied Thermal Engineering* 102: 695-700.

[22] Wang G., Wang F., Shen F., Chen Z., and Hu P., 2019. Novel design and thermodynamic analysis of a solar concentration PV and thermal combined system based on compact linear Fresnel reflector. *Energy* 180: 133-148.

[23] Lokeswaran S., Mallick T.K., and Reddy K., 2020. S. Design and analysis of dense array CPV receiver for square parabolic dish system with CPC array as secondary concentrator. *Solar Energy* 199: 782-795.

[24] Helmers H., Bett A.W., Parisi J., and Agert C., 2014. Modeling of concentrating photovoltaic and thermal systems. *Progress in Photovoltaics: Research and Applications* 22(4): 427-439.

[25] Renno C., D'Agostino D., Minichiello F., Petito F., and Balen I., 2019. Performance analysis of a CPV/T-DC integrated system adopted for the energy requirements of a supermarket. *Applied Thermal Engineering* 149: 231-248.

[26] Aprea C. and C. Renno. 1999. An air-cooled tube-fin evaporator model for an expansion valve control law. *Mathematical Computer Modelling* 30: 135-146.